Sustainable Water Resources Management (2025) 11:50
https://doi.org/10.1007/s40899-025-01228-1

ORIGINAL ARTICLE

Evaluating landuse and climate change effects on current and future hydrologic response and its economic valuation in a North-Indian basin using SWAT

Meraj Alam Ansari[1] · Natesan Ravisankar[1] · Himanshu Joshi[2] · Meenu Rani[1] · Mohammad Shamim[1] · Adlul Islam[3] · Ashisa K. Prusty[1] · Raghavendra K. J.[1] · Raghuveer Singh[1] · Sunil Kumar[1] · Azad S. Panwar[1]

Received: 13 November 2024 / Accepted: 13 March 2025

Abstract

The study assesses the hydrological responses of a major sub-basin in the Upper Ganga Basin, Uttar Pradesh, India, focusing on the effects of land use changes and climate change (CC) impacts. SWAT and General Circulation Models were used to assess the water yields under current (2020) and future scenarios (2030 & 2050), particularly considering the impacts of organic farming (OF) and agroforestry (AgF) practices. Despite theoretical expectations, the results indicate only minor changes in water yield between different policy scenarios (Business-as-Usual, Optimistic, and Pessimistic), particularly over shorter timeframes. This limited impact is primarily due to the small scale of land transitioning to OF and AgF, the spatial concentration of these practices, and the dominant influence of climate variables on hydrological outcomes. The presented work then extends to estimating the district-wise hydrological response and its valuation for Meerut, Bulandshahr, Aligarh, and Mirzapur following the considered policies. The economic valuation of water yield across the target districts underscores the need for district-specific interventions to optimize water resource management. The findings suggest that scaling up sustainable practices, integrating advanced climate projections, and continuous monitoring are essential for developing resilient water resource management strategies. The study provides a foundation for future research to explore more extensive and long-term impacts of land use and CC on hydrological systems, with a focus on integrating socio-economic factors to achieve future water sustainability.

Keywords Hydrological response · Organic farming · Agroforestry · SWAT · GCM · Economic valuation

Introduction

The assessment of streamflow response is a prerequisite before executing any water resource development program. Whether it involves building a reservoir, improving irrigation infrastructure, or executing any ecosystem conservation & management project, the quantification of hydrological response is essential in determining their course of action and orientation (Singh and Saravanan 2020). The two factors that principally govern the hydrological response of any drainage system are land use and climate. Land use change has significant effects on hydrology, altering water availability, flow patterns, and quality. Urban expansion typically leads to increased surface imperviousness, often causing more frequent and intense flooding (Arnold and Gibbons 1996; Pickett et al. 2004). While, agricultural practices and expansion, especially in forested regions, can cause reduced interception, transpiration, and decreased baseflow (Allan 2004; Foley et al. 2005). Similarly, climatic factors such as changes in precipitation patterns affect the surface/sub-surface flow (Trenberth et al. 2003), while temperature changes influence time to peak, streamflow patterns, etc.

✉ Meraj Alam Ansari
merajiari@gmail.com

✉ Himanshu Joshi
himanshujoshiphy@gmail.com

[1] ICAR-Indian Institute of Farming Systems Research, Modipuram, Meerut, Uttar Pradesh 250110, India

[2] G. B. Pant National Institute of Himalayan Environment, Kosi-Katarmal, Almora, Uttarakhand 263643, India

[3] NRM Division, Krishi Anusandhan Bhawan-II, ICAR, New Delhi 110012, India

Published online: 05 April 2025

(Kundzewicz et al. 2007). The climate change (CC) impacts also morph the frequency and intensity of weather events (Hirsch and Ryberg 2012; Sheffield et al. 2012). This makes the accounting of CC impacts and land use changes crucial in streamflow response prediction studies (Zhang et al. 2015; Mosbahi et al. 2023). The CC impacts can be integrated into models to understand possible implications on the water resources. Future predictions in the sect of hydrological studies find direct applications in (i) Forecast of streamflow and flood inundation (Cloke and Pappenberger 2009), (ii) Water supply management aspects such as future water availability for developing sustainable strategies for allocation and infrastructure (Gassman et al. 2007), (iii) Identification of drought-prone regions and implementation of apt mitigation measures (Wilhite 2000), (iv) Optimization of reservoir inflows, estimation of losses, demand pattern, etc. (Loucks and Van Beek 2005), (v) Ecosystem management such as assessing impact of water management practices on aquatic ecosystems, ecological flow requirements, etc. (Arthington et al. 2006), and (vi) Designing of CC impact resilient infrastructure and adaptation strategies.

Over the last five decades, hydrologic models have been extensively used to estimate streamflow attributes. A hydrologic model approximates a real-world hydrologic system, e.g., lake, river, estuary, etc., whose inputs and outputs are hydrologic variables linked via some set of equations. At the core of the model lies the concept of system transformation (Chow et al. 1988). In the case of river systems, hydrologic modeling may be typically narrowed down to comprehend the behavior of the surface and the subsurface that influences the streamflow characteristics (Parajuli and Ouyang 2013). In data-scarce drainage systems, hydrologic modeling has produced competent baseline information and deduced long-term effects that are otherwise very hard to articulate (Altaf et al. 2013). Hydrologic models can simulate and forecast both the qualitative and quantitative aspects of water emanating at the outlet of a drainage system, thus, aiding policy and decision-makers in accomplishing desired goals (Lüke and Hack 2018). One such model is the Soil and Water Assessment Tool (SWAT), a continuous, public-domain model functioning at daily time steps using process-based equations. The model, following multiple adaptations since its inception, has proven useful in hydrologic modeling under diverse climatic conditions and topographical footings (Krysanova and Arnold 2008; Tuppad et al. 2011; Yuan et al. 2015; Zhang et al. 2020). It is widely used for assessing the impact of land management practices on water resources. The model can simulate various hydrologic indices such as surface runoff, evapotranspiration, groundwater flow, etc. (Neitsch 2011). SWAT, also, provides a large user base and detailed instruction manuals over diverse hydrologic landscapes, thus allowing new users to quickly familiarize themselves with various model processes (Jain et al. 2017). Further, the easy integration of SWAT over existing Geographical Information System (GIS) software like ArcGIS, QGIS, etc., makes it more preferred among the hydrologic modelers.

Multiple attempts have been made in the last two decades to quantify the effects of changes on land use and the climate over hydrological responses (Niraula et al. 2015; Soman & Chithra 2019). However, a critical research gap remains in evaluating both factors simultaneously within a predictive framework that integrates observed climatic conditions and General Circulation Models (GCMs). While past research has often examined land use or climate influences in isolation, relatively few studies have coupled these factors to predict long-term hydrological responses in large drainage systems (Hyandye et al. 2018; Chen and Chang 2020; Haleem et al. 2022; Kumar et al. 2022; Mosbahi et al. 2023). Additionally, most SWAT-based studies are site-specific, limiting their applicability for policy-driven water management at regional or national levels. Moreover, even less considers the economic accounting of water yield, especially over administrative boundaries such as blocks, districts, etc., under such studies. The presented study is an attempt in this direction that aspires to integrate SWAT with the current climatic data and a suitable GCM (MICRO5) for prediction of future hydrological responses in a sub-basin, namely, Upstream of Gomti Confluence to Muzaffarnagar (USGCM), of the Upper Ganga Basin (UGB). SWAT alone cannot account for climate variability beyond the historical period, making its integration with land use change scenarios and GCMs essential. GCMs provide future climate projections such as precipitation trends, temperature changes, extreme weather events, etc., and SWAT relies heavily on meteorological and land use inputs. Therefore, integration of SWAT with suitable GCM and land use scenarios allows for future-oriented hydrological modeling ensuring accounting of both anthropogenic and climatic drivers. Administratively, the entire study area lies in the state of Uttar Pradesh, India. The study takes into account the changing land use patterns, especially the dynamics of organic farming (OF) and agro-forestry (AgF) under three policies. Further, the deliberated study provides estimates of water yield and its valuation for the 04 districts of Uttar Pradesh (UP) following the weighted-area method for the present and future scenarios under the diverse land use scenarios. The study is significant in the sense that it (i) Conducts a basin-scale assessment, ensuring findings are applicable beyond district-level management, (ii) Integrates land use transitions (OF and AgF) with CC projections, offering a more comprehensive long-term hydrological outlook, and (iii) Provides economic valuation of water yield, linking hydrological changes to tangible economic impacts at a regional scale.

Given the geographical extent of the study area, the study findings are non-local and hold relevance for other semi-arid and intensively cultivated river basins worldwide.

Additionally, the contemplated work finds its linkages with several national and international initiatives, including India's Nationally Determined Contribution (NDC) 1 (Mission Lifestyle for Environment (LiFE)) and 6 (To better adapt to CC by enhancing investments in development programs in sectors vulnerable to CC) under the Paris Agreement (2016) at United Nations Framework Convention on Climate Change, and the recently launched Green Credit Program (water and sustainable agriculture-based green credits) of Ministry of Environment Forest & Climate Change (MOEFCC), Government of India (GOI). Further, it is also crosscutting several Sustainable Development Goals (SDGs) of the United Nations (UN), viz., SDG 6-Clean water & sanitation (6.4–6.6), SDG 13-Climate action (13.1 & 13.2), and SDG 15-Life on land (15.1 & 15.3), respectively.

Material and methods

Study area

The USGCM has a geographical extent of 31,289.76 sq. km, extending from latitude 24.862° N to 29.478° N and longitude 77.528° E to 83.119° E, and with a periphery of 3924.2 km. It is a part of UGB and houses twenty (20) watersheds from GNGT001 to GNGT020 (CGWB 2006). The absolute relief of the drainage system varies from 320 to 11 m AMSL, with an average elevation of 133.2 m Above Mean Sea Level (AMSL). Following the Strahler classification USGCM is an eighth-order drainage system. From the headwaters of USGCM (located in the Muzaffarnagar district) originate the Kali Nadi. This river courses southeast until Kannauj, where it meets the Ganges and later with the Ramganga River (R.) Further, proceeding towards the southeast, the river converges with the Yamuna R. at Prayagraj. The outlet of the USGCM is located in the Varanasi district of UP. The geomorphology of the study area features older alluvial plains, older flood plains, and moderately dissected structural lower plateaus. Additional geomorphic elements include low-dissected structural & moderately dissected denudational lower plateaus, active flood plains, pediment pedi-plain complexes, and waterbodies. The predominant lithological composition of the AOI consists of oxidized silt clay with *kankar* and micaceous sand. Additionally, five categories of lineaments, namely break in slope, drainage parallel, fault, joint/ fracture, and scarp parallel, can also be identified within the drainage system. One of the major objectives of the conferred study is to estimate water yield responses from the administrative boundaries of 04 districts of UP, namely, Aligarh, Bulandshahr, Meerut, and Mirzapur. As the USGCM is the only sub-basin in the UGB that lies within the periphery of UP and covers major land parcels of all these districts, hence it was selected as the study area. Figure 1 illustrates the index map of the USGCM along with the location of the target districts.

Development of sub-watersheds and drainage network

The conferred study utilized SWAT 2012 in conjunction with ArcGIS version 10.4.1, employing 82 Survey of India Open Series Maps, with sheet numbers 53G, 53H, 53L, 54I, 54 M, 54N, 63A, 63B, 63C, 63F, 63G, 63 K, 63L, and 63O, to develop the drainage network for the AOI. Further, the ASTER Global Digital Elevation Model (GDEM) Version 3 served as the input to SWAT for the delineation of boundaries of the sub-watersheds and the entire drainage system. The'Automatic Watershed Delineation' with 10 user-defined sub-outlets & 05 inlets and the prepared drainage network was employed for this purpose. Finally, A total of 11 sub-watersheds, namely, SW1 to SW11, were developed. Three (03) inlets were marked at watersheds GNRM049, RMGG027, and RMGG026 in the central portion which denotes the influxes from Ganges R. before the confluence of Ramganga R. and from the Ramganga sub-basin, while, two (02) inlets were pinned at TONS023 and the junction of GNGT020 and GNGT016 indicating the contributions from Tons and Yamuna R. In regards to the sub-outlets/ outlets, administrative boundaries of districts Meerut, Bulandshahr, and Aligarh were used for the delineation of sub-basins SB1, SB2, SB3, and SB4, while the district boundary of Mirzapur towards the rendition of SB10 and SB11, respectively. The other sub-outlets are located at the junction of GNGT007 & GNGT006 for SB5, GNGT008 & GNGT009 for SB6 and SB7, and GNGT010 & GNGT002 for SB8, respectively. SB9 houses the main outlet of the drainage system. Figure 2 depicts the developed sub-watersheds and the drainage network.

Soil, slope, and land use definition

For the development of the soil map, the Digital Soil Map of the World (DSMW) of the Food & Agriculture Organization (FAO) of scale 1:250,000 was used. The vector soil map was converted into a raster with a projected coordinate system (UTM WSG 1984 Zone 44 N). For the slope map slope classes as per the recommendations of Kumar and Kushwaha (2013) were taken into account. As SWAT allows a maximum of five (05) slope classes, some of the slope classes (corresponding to higher slopes) were clubbed

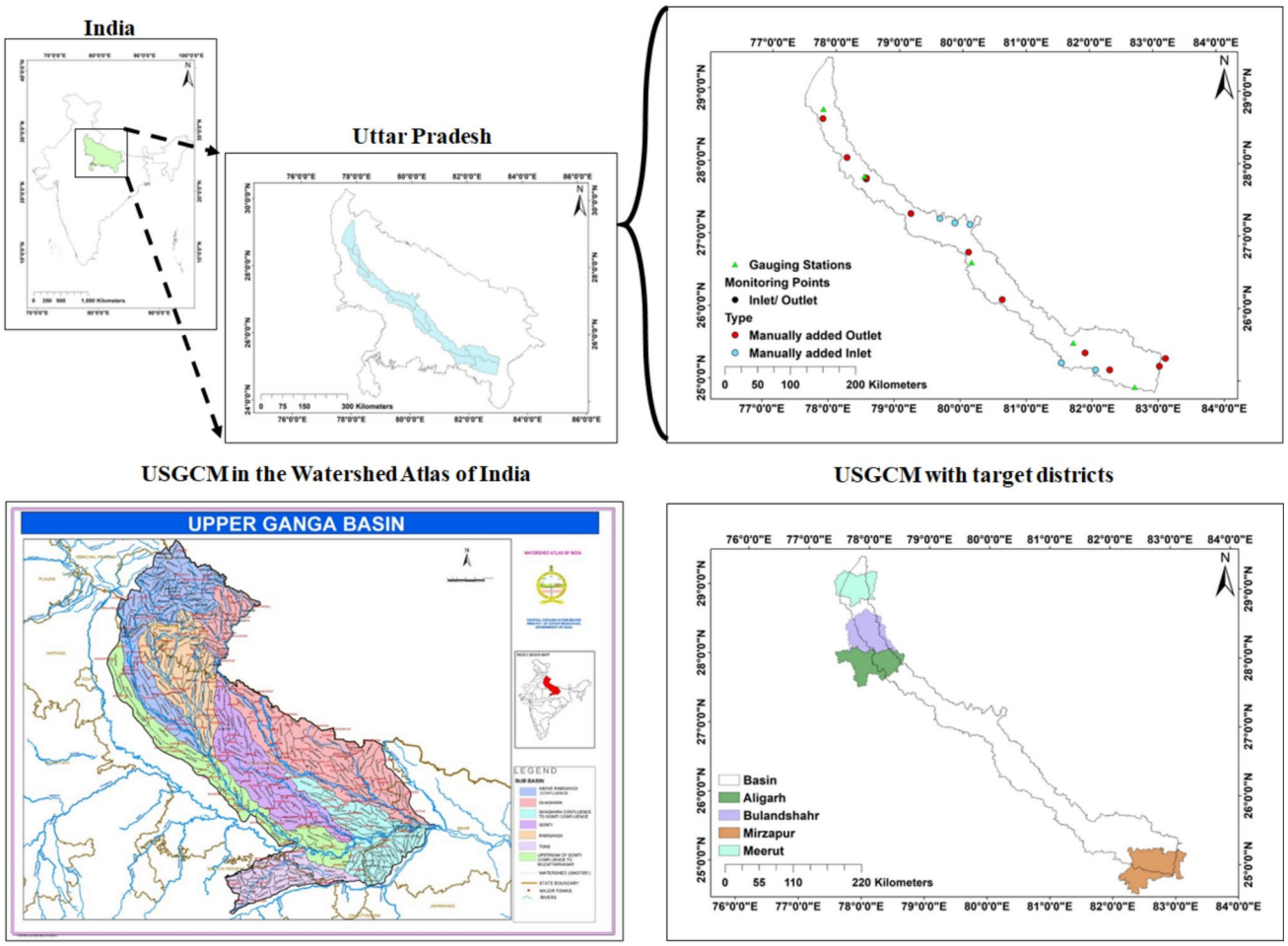

Fig. 1 Index map with inlets/ outlets and target districts

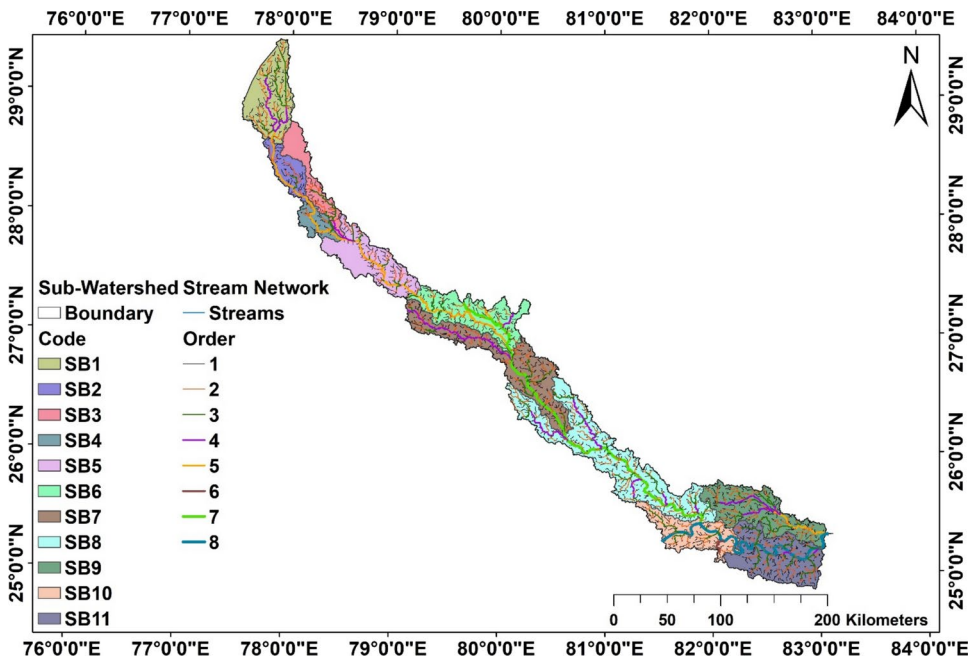

Fig. 2 Sub-watersheds and the drainage network

together. The developed classes were (i) Nearly level (0 to 2%), (ii) Gently undulating (2 to 4%), (iii) Strongly undulating (4 to 6%), (iv) Gently rolling (6 to 10%), and (v) Higher (>10%) including strongly rolling, hilly, steep, very steep, and extremely steep.

For land use, a total of 13 maps were prepared. The first corresponds to the year 2020, for which Sentinel-2A data of spatial resolution 10 m was used. The remaining 12 future land use maps were developed from 06 land use scenarios sets which were the outcomes of 03 sets of policies, namely, Business as Usual (BaU), optimistic & pessimistic, coupled with 02 Representative Concentration Pathways (RCP) projections, viz., 4.5 & 8.5, for the years 2030 & 2050. The BaU conforms with the expansion of OF @ 10% per year along with 10% of the total cropped land under AgF, while the optimistic policy accords with growth in OF @ 15% per year with 33% of the arable parcels under the AgF, respectively. The pessimistic policy corresponds to the reduction in the expansion of OF @ 5% per annum with no change in the area under AgF. The scenario developed from (BaU+RCP 4.5) was abbreviated as S_1, while (BaU+RCP 8.5) was categorized as S_2. Similarly, the (Optimistic+RCP 4.5), (Optimistic+RCP 8.5), (Pessimistic+RCP 4.5), and (Pessimistic+RCP 8.5) were abbreviated as S_3, S_4, S_5, and S_6, respectively. The future land use data for these scenarios of spatial resolution 1 sq.km was extracted from the Data Centre for Resources and Environmental Sciences of the Chinese Academy of Sciences (Chen et al. 2020). The developed soil, slope, and land use maps were resampled and lookup tables (in.txt format) for soil and land use classes were prepared and imported to the SWAT model.

Input hydro-meteorological data

The input files are prepared in.txt format with their respective look-up tables containing the location (lat., long., and elevation) of the station/ gauging point and the.txt file name containing the meteorological data. For the study area, a total of 05 gauging sites/ points were selected. For the initial run meteorological data from 2000 to 2020 was consummated at daily steps from the NASA Prediction of Worldwide Energy Resources (POWER) Langley Research Center (LaRC). For RCP projections (4.5 & 8.5), three (03) daily meteorological indices, namely, precipitation (pr), air temperature (tasmax and tasmin), and wind speed (sfcWind) were amassed from World Climate Research Program (WCRP), Dept. of Energy, Lawrence Livermore National Laboratory using MIROC5 GCM following the recommendations of Mishra et al. (2014) and Sharmila et al. (2015). The RH for the RCP projections was derived using the specific humidity (huss), mean air temperature (tas), and sea level air pressure (psl) data. The psl values are converted to air pressure (ps) using the elevation of the gauging location following FAO recommendations (Eq. 1), and then RH is derived using the Clausius-Clapeyron (Chang 2013) via Eq. 2.

$$\mathrm{ps} = \mathrm{psl}\left[\frac{293\text{-}0.0065\mathrm{z}}{293}\right]^{5.26} \tag{1}$$

where z is the elevation (m) from mean sea level

$$\mathrm{RH}\ (\%) = (0.263.\mathrm{ps.huss})\mathrm{e}^{\left[\frac{17.27(\mathrm{tas}-273.15)}{\mathrm{tas}-29.75}\right]^{-1}} \tag{2}$$

where tas is in Kelvin (K)

For RCPs, the meteorological data at daily time scales is taken from 2020 to 2050.

Model calibration and validation:

Model calibration and validation were accomplished using the SWAT-Calibration and Uncertainty Program (CUP) using NASA Global Land Data Assimilation System (GLDAS)-2.2 data on baseflow-groundwater runoff and storm surface runoff of 0.25° spatial resolution at monthly timescales from 2004 to 2020. In the SWAT-CUP Sequential Uncertainty Fitting (SUFI)-2 algorithm was used for calibration as it considers all sources of uncertainty under parameter uncertainty (Abbaspour 2015). The objective function used for the calibration is to maximize the Nash–Sutcliffe Efficiency (NSE) and is stated in Eq. (3). Besides NSE, percent bias (PBIAS), and Root Mean Squared Error (RMSE)-Observation Standard Deviation ratio (RSR) were also used as the model performance indicators (Eqs. (4) and (5)). The recommended thresholds as provided by Moriasi et al. (2007) and Abbaspour et al. (2015) on NSE, PBIAS, and RSR were used, which consider a streamflow model as satisfactory if NSE>0.5, PBIAS≤±25, and RSR≤0.70.

$$\text{Maximize: NSE} = 1 - \frac{\sum_{\mathrm{i}}\left(\mathrm{Q_m} - \mathrm{Q_s}\right)^2}{\sum_{\mathrm{i}}\left(\mathrm{Q_{m,i}} - \bar{\mathrm{Q}}_{\mathrm{m}}\right)^2} \tag{3}$$

$$\mathrm{PBIAS} = 100 * \frac{\sum_{\mathrm{i}=1}^{\mathrm{n}}\left(\mathrm{Q_m} - \mathrm{Q_s}\right)_{\mathrm{i}}}{\sum_{\mathrm{i}=1}^{\mathrm{n}}\mathrm{Q_{m,i}}} \tag{4}$$

$$\mathrm{RSR} = \frac{\left[\sqrt{\sum_{\mathrm{i}}\left(\mathrm{Q_m} - \mathrm{Q_s}\right)_{\mathrm{i}}^2}\right]}{\left[\sqrt{\sum_{\mathrm{i}}\left(\mathrm{Q_{m,i}} - \bar{\mathrm{Q}}_{\mathrm{m}}\right)^2}\right]} \tag{5}$$

where Q_m is the measured runoff (baseflow + storm surface runoff), Q_s is the simulated runoff (SWAT simulated), and $\bar{Q}_m$ is the average value of the measured runoff. A sensitivity analysis (following the global sensitivity approach) was also conducted towards the identification of the most influential parameters that affect the model's predictions, allowing for a more focused and efficient calibration process (Abbaspour et al. 2007; Arnold et al. 2012). Table 1 depicts various data sources used for the hydrological modeling and subsequent validation of the developed model.

Estimation of district-wise hydrologic response and its valuation

Estimating district-wise hydrological responses is particularly challenging, as administrative boundaries rarely align with natural drainage basins. Unlike watershed-based hydrological assessments, district-level estimates require spatial disaggregation techniques to link hydrological response units with administrative divisions (Gassman et al. 2007). To achieve this, the area-weighting method was applied in this study, ensuring that hydrological responses from sub-basins could be apportioned to districts in a systematic manner. Two key assumptions were made to facilitate this estimation. The first one was the uniform response distribution assumption under which each sub-basin's hydrological response was assumed to be evenly distributed across its geographical extent. This assumption aligns with previous SWAT-based sub-basin response allocation studies where hydrological fluxes are considered spatially homogeneous within individual sub-basins (Rostamian et al. 2008; Schuol et al. 2008). The second was proportional area contribution approach which distributes sub-basin responses across overlapping administrative units following a normalized area-weighting technique (Immerzeel et al. 2010). The fraction of each sub-basin's area falling within a target district was first normalized against the total area of the respective sub-basin. This fraction was then multiplied by the total district area to obtain a compounded areal value representing the district's hydrological contribution. Then the per-unit response of the concerned sub-basin was multiplied by this compounded area factor to estimate the district's overall hydrological response. This formulation is commonly used in hydrological modeling where administrative-level hydrological estimates are needed but do not directly align with watershed delineations (Wagner et al. 2011). As a result, Eqs. (6)–(9) were developed.

$$R_{Meerut} = (0.897)\, R_{SB1} \tag{6}$$

$$R_{Bulandshahr} = 1.7768\,(0.026R_{SB1} + 0.05201R_{SB2} + 0.445R_{SB3} + 0.0088R_{SB4}) \tag{7}$$

$$R_{Aligarh} = 2.7228\,(0.3135R_{SB3} + 0.5756R_{SB4} + 0.1109R_{SB5}) \tag{8}$$

$$R_{Mirzapur} = 1.275R_{SB11} \tag{9}$$

where R_{SBi} is the hydrological response of a sub-basin and $R_{District}$ is the response for the respective target district. The coefficients represent the normalized area-weighted contributions of each sub-basin to the target district. Finally, to assess the economic value of the estimated hydrological response, the water pricing approach was adopted, considering a unit valuation of INR 18.43 per cubic meter (Verma et al. 2017). Figure 3 illustrates the adapted methodology for the deliberated study.

Table 1 Data sources employed in the study

Parameter	Data source	Details/ remarks (if any)
Topography	ASTER GDEM version 3 (available from: https://search.earthdata.nasa.gov/search)	Spatial resolution ~ 30 m
Soil	DSMW, FAO, UN	Scale 1:250,000
Land use	Current (2020): Sentinel-2A (available from: https://www.arcgis.com/apps/instant/media/index.html?appid=fc92d38533d440078f17678ebc20e8e2) RCP 4.5 and 8.5 (for 2030 & 2050): GeoSOS (available from: http://www.geosimulation.cn/Global-SSP-RCP-LUCC-Product.html)	Spatial resolution of Sentinel-2A is ~ 10 m and of GeoSOS data is 1 km
Meteorological	2000 to 2020: NASA POWER LaRC (available from: https://power.larc.nasa.gov/data-access-viewer/) RCP 4.5 and 8.5 from 2020 to 2050: WCRP (available from: https://esgf-node.llnl.gov/search/cmip5/)	Temporal resolution: Daily
Storm surface runoff and Baseflow-groundwater runoff	2015 to 2020: NASA GLDAS-2.2 (available from: https://developers.google.com/earth-engine/datasets/catalog/NASA_GLDAS_V022_CLSM_G025_DA1D)	Spatial resolution: 0.25° Used for model calibration and validation

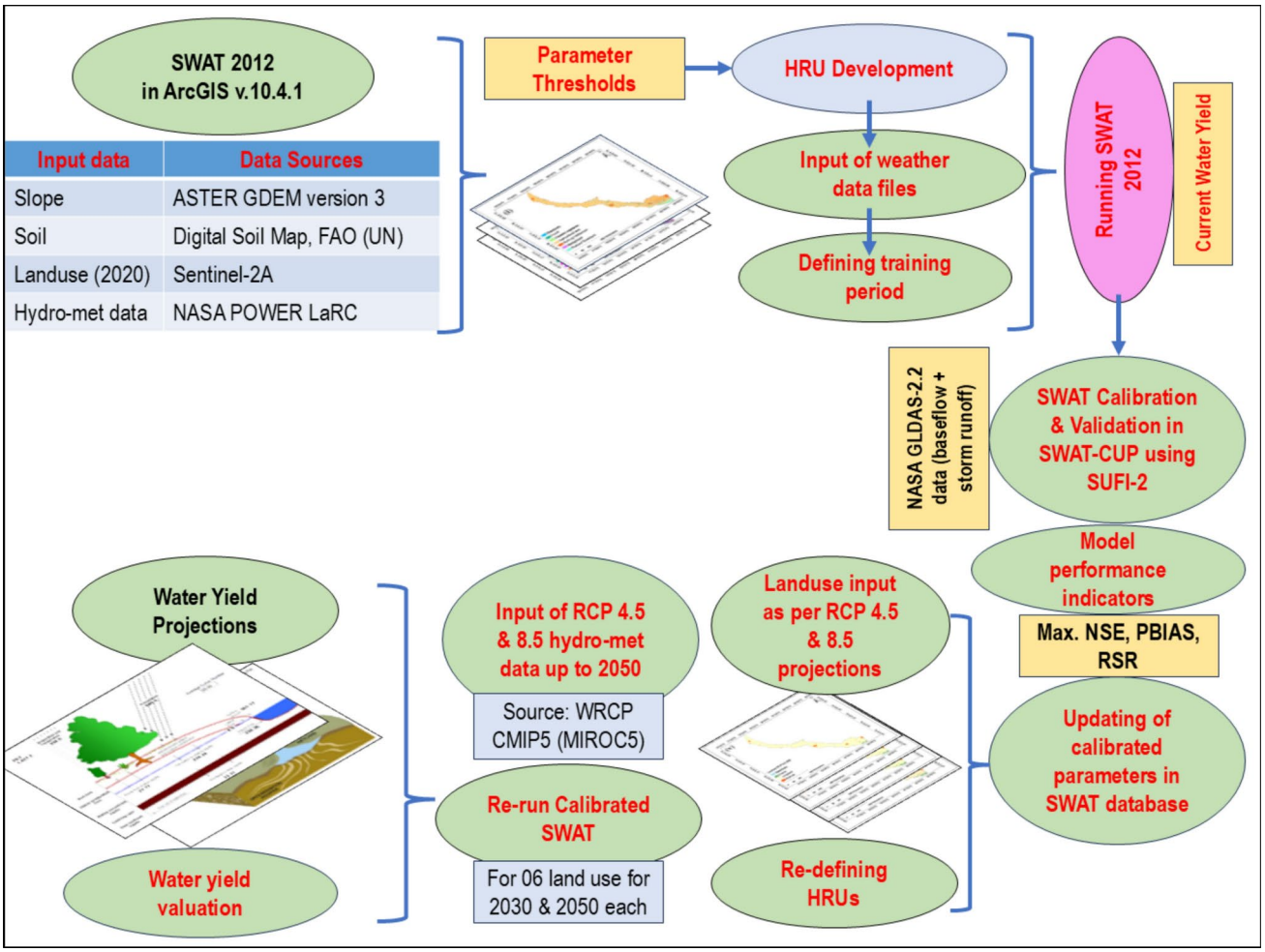

Fig. 3 Adapted methodology

Table 2 Soil classes following DSMW, FAO

SNUM	Area (%)	Area (sq. km)	HSG	Texture class	USLE K-factor	Sand (%)	Silt (%)	Clay (%)
3675	38.18	11,954.59	C	Loam	0.2926	42	36	22
3685	3.27	1023.874	D	Loam	0.2846	41	37	22
3739	5.32	1665.753	D	Loam	0.3077	41	35.5	23.5
3772	0.87	272.4069	D	Sand-clay loam	0.2250	59	17	24
3785	3.49	1092.759	C	Sandy loam	0.2449	71	15	14
3798	5.05	1581.213	D	Loam	0.3053	43	26	21
3810	20.53	6428.177	D	Loam	0.3339	38.5	43.5	18
3812	23.28	7289.233	D	Loam	0.2894	46	32	22

SNUM Soil Number/code, *HSG* Hydrologic soil group, *USLE* Universal soil loss equation

Results and discussion

Soil and slope

In regards to the soil, a total of eight soil types were identified details of which are presented in Table 2. Similarly for slope, five classes as depicted in Sect. "Soil, slope, and land use definition" were developed. These covered 57.59%, 33.91%, 6.24%, 1.77%, and 0.48% of the total drainage area, respectively. Figure 4 illustrates the soil and slope map for the USGCM.

Land use

Seven land use classes, namely, waterbody (1.34%), forest-mixed (1.29%), range/ grassland (4.54%), flooded vegetation (0.01%), cropland (77.97%), moderately dense built-up (14.19%), and bareground (0.66%), were identified for the

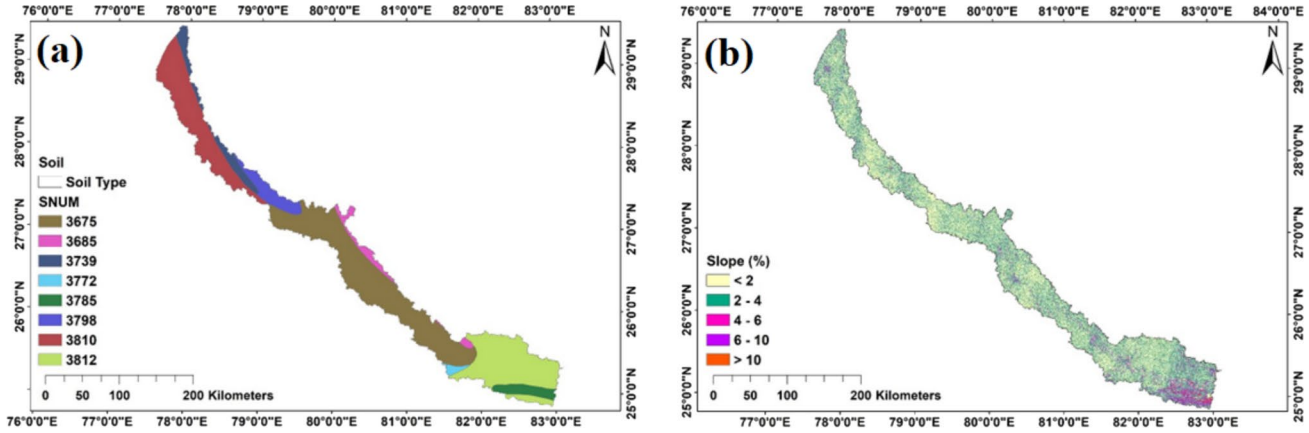

Fig. 4 **a** Soil and **b** Slope map

current scenario (2020). These classes were then assigned suitable land use codes (as per the SWAT database). For the modeling purpose, the flooded vegetation class was excluded due to its negligible proportion. Also, OF and AgF were not separately depicted for 2020 due to their lower relative contribution to the total cropland area. In the context of future land use (2030 & 2050) under BaU, optimistic, and pessimistic policies, OF, and AgF were considered due to relatively higher allocation in the cropland. As a result, separate additions of plant growth parameters such as HVSTI, BLAI, FRGRWM, etc., were made based on the recommendations of ICAR-CAFRI (2016), Lai et al. (2020), ICAR-IIFSR (2021), Čerkasova et al. (2023), Rahman et al. (2023), and Tadesse et al. (2023) for these two classes in the SWAT database. The current (2020) and future land use maps for 2030 & 2050 are provided as supplementary material and the percentage under various land use classes is depicted in Table 3.

Development of hydrologic response unit

A Hydrologic Response Unit (HRU) is a fundamental spatial unit of the model, following a distinct combination of land use, slope, and soil, as per user-defined thresholds. For defining the HRU, a threshold value of 1%, 2%, and 2% were used for land use, soil, and slope class, respectively. For 2020 285 complete HRUs were developed, while for 2030 the number of HRUs in S_1, S_2, S_3, S_4, S_5, and S_6 scenarios were 210, 219, 220, 226, 206, and 215, respectively. Similarly, for 2050 these were 278, 294, 282, 311, 206, and 234, respectively. Further, no elevation bands were developed for the given modeling scenario as the study area has no snow cover nor it does have large basin relief.

SWAT simulations, model calibration, and validation

Initial simulation in SWAT was executed from 2000 to 2020 at monthly time steps with the first four years (2000–2003) as the warm-up period (NYSKIP). The model results were then exported to SWAT-CUP for calibration & validation. Before commencing calibration, the initial feasibility of the SWAT model was evaluated using the model performance indicators following a dummy iteration with a single simulation. *r_SFTMP.bsn* was used as the dummy parameter with a range of 0 to 0. NSE, PBIAS, and RSR for the dummy iteration were 0.74, 38.4%, and 0.51, respectively. Further, the modified coefficient of determination (bR^2) was estimated at 0.6002. The PBIAS is out of range of what is recommended by Moriasi et al. (2007) and Abbaspour et al. (2015). This relatively larger PBIAS suggests that the SWAT model is underpredicting the observed streamflow (Gupta et al. 2009) commending for model calibration. A hydrograph for the dummy iterations is provided as the supplementary dataset.

For model calibration monthly observed streamflow from 2004 to 2015 was used. Under model parameterization (*Par_inf.txt*) of SWAT-CUP 14 parameters affecting surface runoff, available water capacity & hydraulic conductivity of soil, slope, groundwater, evaporation, etc., were adjusted using the absolute qualifier. This was followed by the execution of calibration iteration with 500 simulations. Dotty plot of the calibration iteration is provided in the supplementary material. The best NSE, PBAIS, and RSR from the calibration iteration were 0.85, 23.6%, and 0.39, while the bR^2 was estimated at 0.6960 suggesting the model performed well in predicting the observed streamflow. Table 4 illustrates the fitted value of model parameters along with the results of global sensitivity analysis (p-value & t-stat). Under the global sensitivity method parameter sensitivities are computed following a multiple regression equation. Parameters generated via latin hypercube are regressed against the

Table 3 Relative proportion (in %) of different classes in the future land use scenarios

Landuse class	2030						2050					
	S1	S2	S3	S4	S5	S6	S1	S2	S3	S4	S5	S6
Waterbody	1.73	1.73	1.73	1.73	1.73	1.73	1.73	1.73	1.73	1.73	1.73	1.73
Forest (mixed)	2.32	1.47	2.32	1.47	2.32	1.47	2.02	0.92	2.02	0.92	2.02	0.92
Rangeland	0.00	NA	0.00	NA	0.00	NA	NA	NA	NA	NA	NA	NA
Barrenland	0.03	0.00	0.03	0.00	0.03	0.00	NA	NA	NA	NA	NA	NA
Cropland	87.62	87.83	88.56	74.87	88.38	88.67	84.31	85.26	61.60	61.57	88.09	88.92
Built-up	1.73	2.06	1.73	2.06	1.73	2.06	2.01	2.80	2.01	2.80	2.01	2.80
Organic farming	0.47	0.45	0.66	0.64	0.11	0.15	3.41	3.00	12.44	12.46	0.05	0.01
Agroforestry	6.09	6.44	4.97	19.22	5.69	5.92	6.51	6.28	20.19	20.52	6.09	5.62

NA: Not applicable

Table 4 Fitted value, t-stat, and *P*-value of adjusted parameters in SWAT-CUP

Parameter name	Parameter qualifier & code	Fitted value	t-Stat	*P*-value
SCS runoff curve no	v__CN2.mgt	86.32	8.602	0.000
Available water capacity of the soil layer	v__SOL_AWC().sol	0.04	−52.171	0.000
Average slope length	v__SLSUBBSN.hru	73.99	−0.586	0.558
Saturated hydraulic conductivity	v__SOL_K().sol	330.50	1.411	0.159
Soil evaporation compensation factor	v__ESCO.hru	0.30	1.639	0.102
Manning's "n" value for overland flow	v__OV_N.hru	0.26	0.569	0.570
Threshold depth of water in the shallow aquifer required for return flow to occur (mm)	v__GWQMN.gw	773.80	−2.341	0.020
Groundwater "revap" coefficient	v__GW_REVAP.gw	0.01	−105.960	0.000
Threshold depth of water in the shallow aquifer for "revap" to occur (mm)	v__REVAPMN.gw	268.70	−1.244	0.214
Effective hydraulic conductivity in main channel alluvium	v__CH_K2.rte	260.90	−0.720	0.472
Plant uptake compensation factor	v__EPCO.hru	0.16	0.399	0.690
Baseflow alpha factor (days)	v__ALPHA_BF.gw	0.83	3.587	0.000
Maximum canopy storage	v__CANMX.hru	2.93	0.948	0.344
Groundwater delay (days)	v__GW_DELAY.gw	46.26	−6.789	0.000

objective function. This is followed by a t-test determining the relative significance of each parameter. The larger the absolute value, i.e., the value of the t-test, and the smaller the *p*-value, the more sensitive the parameter. The most sensitive parameters were the groundwater 'revap' coefficient, available water capacity, and average curve number. These all have a *p*-value of 0.000 while their absolute t-stat is 105.960, 52.171, and 8.602, respectively. This means that the adjustments to these parameters will have a significant impact on the model's performance (Abbaspour et al. 2007). For validation monthly streamflow data from 2016 to 2020 was used. The fitted values of the adjusted parameters were updated in the *Par_inf.txt* file and another iteration with a single simulation was executed in SWAT-CUP. NSE, PBAIS, RSR, and bR^2 were observed to be 0.84, 22.5%, 0.40, and 0.7242 suggesting the calibrated model performed well in the validation period also. Figure 5 depicts the observed and simulated hydrographs post-calibration. The calibrated parameters were then updated in the SWAT database either manually or through the 'Manual Calibration Helper'. The updated model was then re-run from 2000 to 2020. For this period the region received an average precipitation of 836.78 (±36.31) mm of which 305.48 (±20.15) mm and 14.27 (±0.56) mm escaped as surface runoff and lateral flow. The groundwater contribution to the streamflow and the amount of water that percolates past the root zone were 239.57 (±11.26) mm and 262.16 (±12.40) mm, respectively. The average water yield was 572.64 (±31.28) mm. Further, 264.25 (±4.77) mm evaded as evapotranspiration (ET). The average curve number for the study area was estimated at 86.92. The water and temperature stress days were 52.56 and 8.45, respectively, suggesting the drainage system is a low-stressed watershed following the classification of Ficklin et al. (2012). However, the periodic seasonal water stress may still require adaptive water management strategies. The ratio of streamflow, ET, and percolation to precipitation were 0.67, 0.32, and 0.31, while, baseflow and surface runoff to total flow were 0.45 and 0.55, respectively. Figure 6 illustrates the average monthly water balance from 2000 to 2020.

Prediction of future hydrologic response

The calibrated SWAT model was run from 2020 to 2030 towards the development of 06 scenarios, viz. S_1, S_3, and S_5 for RCP 4.5 and S_2, S_4, and S_6 for RCP 8.5. Likewise, 06 more scenarios were developed for 2020 to 2050. For the year 2030 under RCP 4.5, the average water yield for the S_3 was 596.56 mm which was only 0.57% higher than that of S_1, while for the S_5 it was 590.33 mm which was 0.47% lower than that of S_1. Likewise, for RCP 8.5, the water yield under the S_4 was 587.86 mm, while it is 586.29 mm and 577.14 mm in S_2 and S_6, respectively. It suggests a minuscule increase in water yield (0.27%) following the optimistic policy when compared with BaU. Similarly, for the year 2050 following RCP 4.5, the water yield index for S_3 was

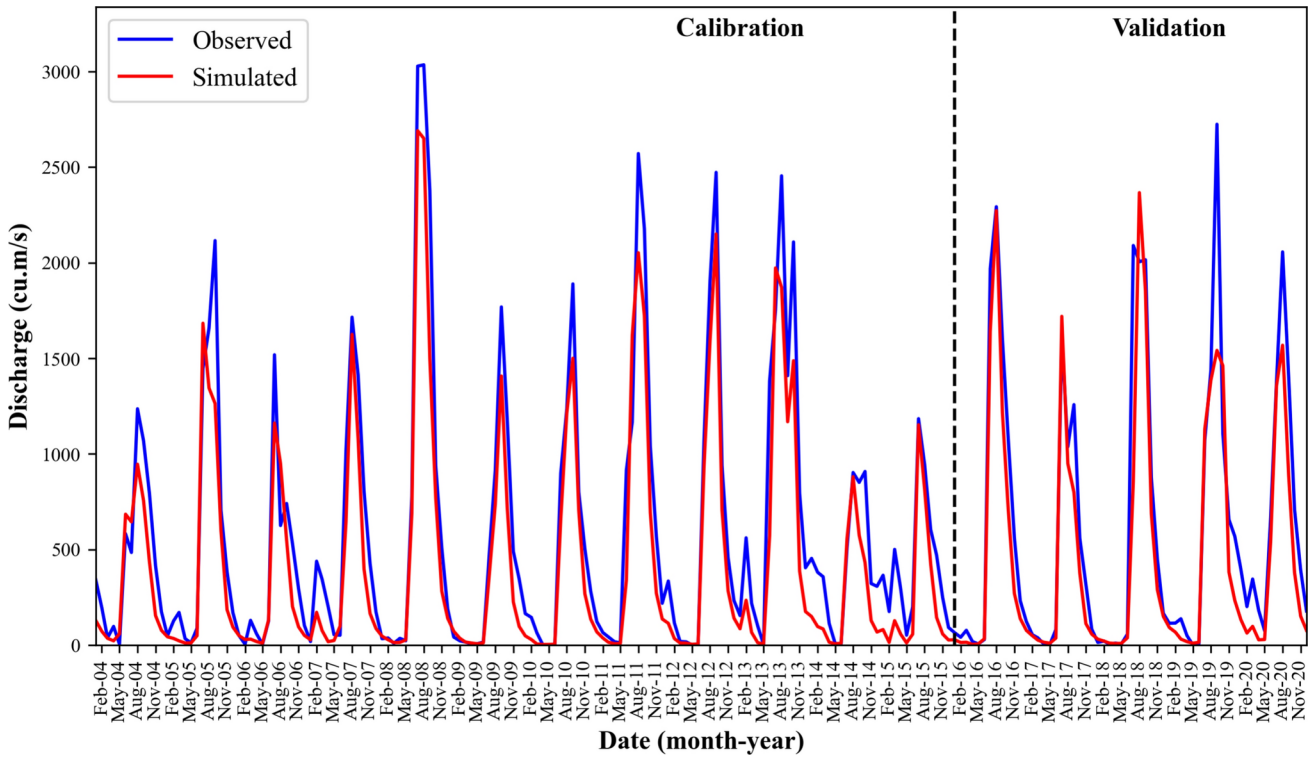

Fig. 5 Observed and simulated streamflow for the best simulation

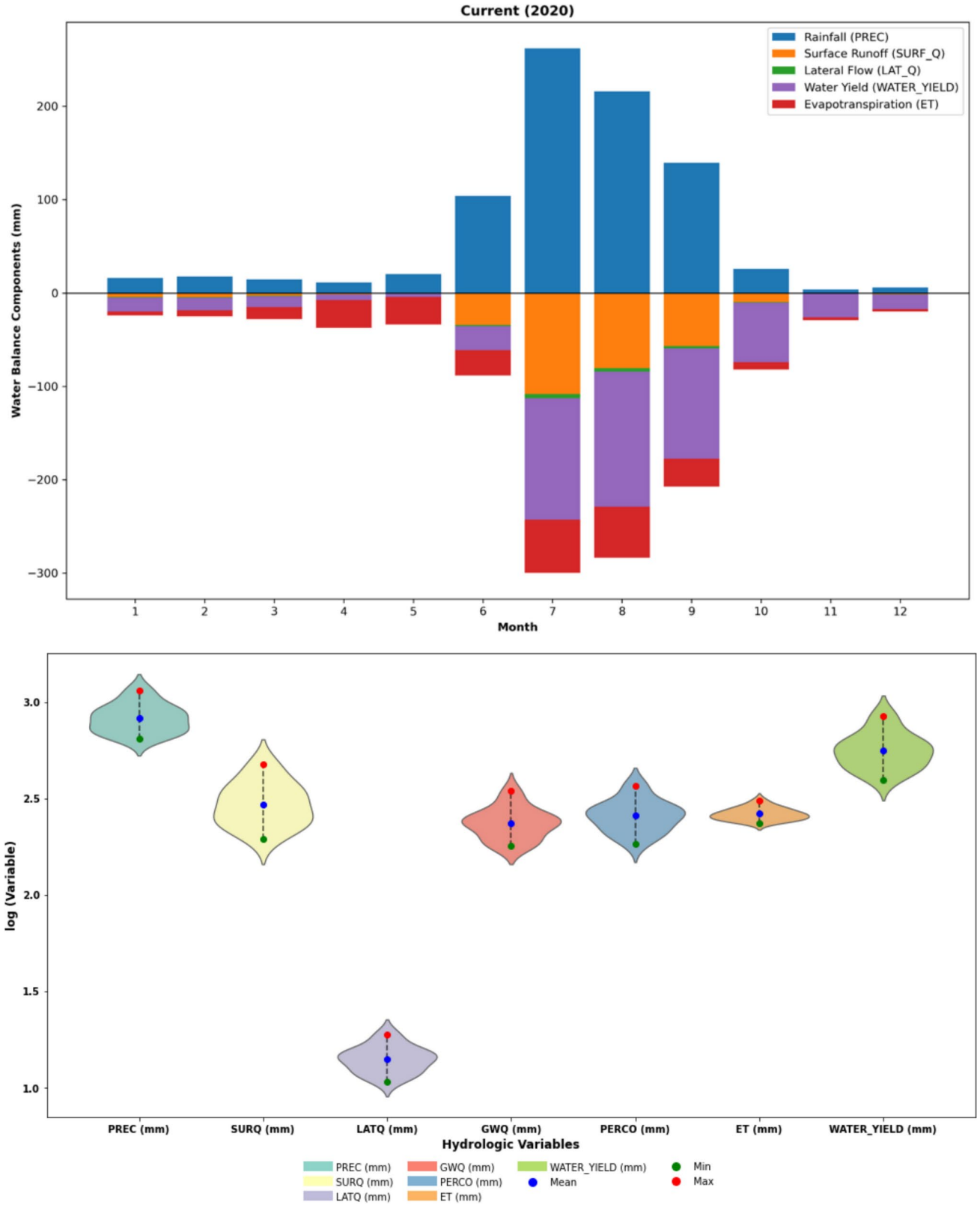

Fig. 6 Average monthly water balance components and dispersion of hydrologic variables from 2004 to 2020 for the calibrated model

703.68 mm, while that for S_1 was estimated at 699.59 mm. In S_5, the water yield was 623.55 mm which is 10.87% lower than that of S_3. Analogously, for 2050 under RCP 8.5 the water yield in S_4 is 668.39 mm which is 1.97% higher than S_2, while for S_6 it is 562.14 mm which is 14.23% lower than S_2, respectively. Table 5 illustrates various hydrologic balance indices for the developed scenarios.

The non-significant changes in the water yield responses for the year 2030 following the optimistic policies when compared to BaU and pessimistic were potentially due to the very low transitioning of arable lands to OF and AgF. Table 3 shows that the area under OF in 2030 is only 0.47%, 0.66%, and 0.11% for the S_1, S_3, and S_5, respectively. Correspondingly, for S_2, S_4, and S_6 it is 0.045%, 0.64%, and 0.15%, respectively. Additionally, given the rates of expansion OF coupled with the short time horizon of 2020–30 is not long enough to capture the full impact of changes in OF and AgF on the water yield. Further, the influence of climatic factors and model assumptions also leads to relatively modest changes in the water yields among the BaU, Optimistic, and Pessimistic scenarios. In 2050, though there is a sizeable difference in water yield between Optimistic and Pessimistic policies the difference in water yield between the Optimistic and BaU is also small despite being a sizeable portion of arable parcels under the OF (12.44% vs. 3.41% for RCP 4.5 and 12.46% vs. 3% for RCP 8.5). These results contrast with what is documented by Azarbad (2022), Wu et al. (2023), Santosha et al. (2024), and Montagnini (2024) where OF and AgF have positively influenced water infiltration, soil moisture retention, water regulation, and overall hydrologic responses in agroecosystems. This potentially is due to the (i) Spatial distribution of land use changes which are not uniformly distributed across the landscape but are instead concentrated in specific areas, the impact on water yield might be localized and not reflected in the overall model results (Kiersch 2000; Schilling and Libra 2003), and (ii) Low model sensitivity to specific land use change as seen in the results of sensitivity analysis (Ghaffari et al. 2010; Winchell et al. 2013). Further, the effects of OF are most pronounced at the field or farm scale where it is practiced, often leading to localized improvements in water infiltration and reduced runoff (Lorenz and Lal 2016). Similarly, the AgF, which integrates trees with crops or pastureland, can improve water retention and reduce surface runoff at the local level. The presence of trees increases soil organic matter, enhances root networks, and can alter microclimates, all of which have direct but localized impacts on hydrological cycles (Jose 2009). Moreover, water yield is substantially influenced by several other factors such as precipitation, ET, proportion of other land covers, etc. The localized nature of OF and AgF practices often modest their influence on the overall water balance (Smith et al. 2004), especially

Table 5 Hydrologic indices for the modelled scenarios

Hydrologic indices	2030						2050					
	S1	S2	S3	S4	S5	S6	S1	S2	S3	S4	S5	S6
Water stress days	37.82	37.91	38.08	37.93	37.55	36.47	37.23	26.61	37.42	27.11	34.77	24.76
Temperature stress days	9.93	11.81	10.56	11.8	9.9	11.44	13.51	15.95	13.84	16.65	10.33	13.07
Avg. curve number	77.91	79.83	78.6	80.26	77.41	77.00	88.61	91.22	88.32	94.41	78.88	80.22
Streamflow to precipitation	0.73	0.72	0.73	0.72	0.73	0.73	0.72	0.65	0.72	0.65	0.72	0.64
Baseflow to total flow	0.4	0.38	0.4	0.38	0.4	0.38	0.38	0.32	0.38	0.32	0.38	0.31
Surface runoff to total flow	0.6	0.62	0.6	0.62	0.6	0.62	0.62	0.68	0.62	0.68	0.62	0.69
ET to precipitation	0.26	0.27	0.26	0.27	0.26	0.26	0.26	0.33	0.25	0.33	0.26	0.34
Percolation to precipitation	0.29	0.28	0.29	0.28	0.29	0.27	0.29	0.23	0.29	0.23	0.29	0.22

for a large drainage system as in this case, particularly if these practices are not widely adopted (Arnold et al. 1998). Figure 7 depicts various water balance components for the developed scenarios.

In the context of sub-watersheds, the greatest response was received from SW9 for all the scenarios except for 2020 where the water yield from SW11 is greater. Though both the sub-watersheds received equal rainfall for 2020 (1084.7 mm) the contribution from groundwater flow (332.18 mm vs. 208.78 mm) and percolation (351.81 mm vs. 327.92 mm) are relatively greater for SW11. Further, the surface runoff component of the SW9 is higher (409.33 mm vs. 386.96 mm). This is mostly due to the greater contribution of land uses that complement delayed water releases such as forest (12.81% vs. 1.86%), waterbody (25.35% vs. 3.25%), and pastures (52.67% vs. 1.98%) in SW11. Further, a sizable portion of the SW11 is sandy loam which compared to loam (which is dominant in SW9) has greater infiltration indices. The lowest response was from SW1 (for S_2, S_3, S_4 & S_5 scenarios in 2030, and S_3 & S_5 in 2050), SW2 (for S_1, S_3 & S_5 in 2030), SW3 (for S_6 in 2030, and S_1, S_2, S_4 & S_6 in 2050), and SW4 (for 2020), respectively. It was mostly due to lower precipitation received over these sub-watersheds for the respective time frame. Figure 8 illustrates the heat map of annual water yield for all the sub-watersheds under different scenarios.

District-wise hydrologic response and valuation

The district responses were estimated based on Eqs. (6)–(9) as depicted in Sect. "Estimation of district-wise hydrologic response and its valuation". In 2020, the distribution of water yield and its corresponding valuation showed a clear hierarchy among the districts. Aligarh had the highest water yield at 1078.73 mm, followed by Mirzapur with 981.26 mm. Bulandshahr and Meerut had lower yields at

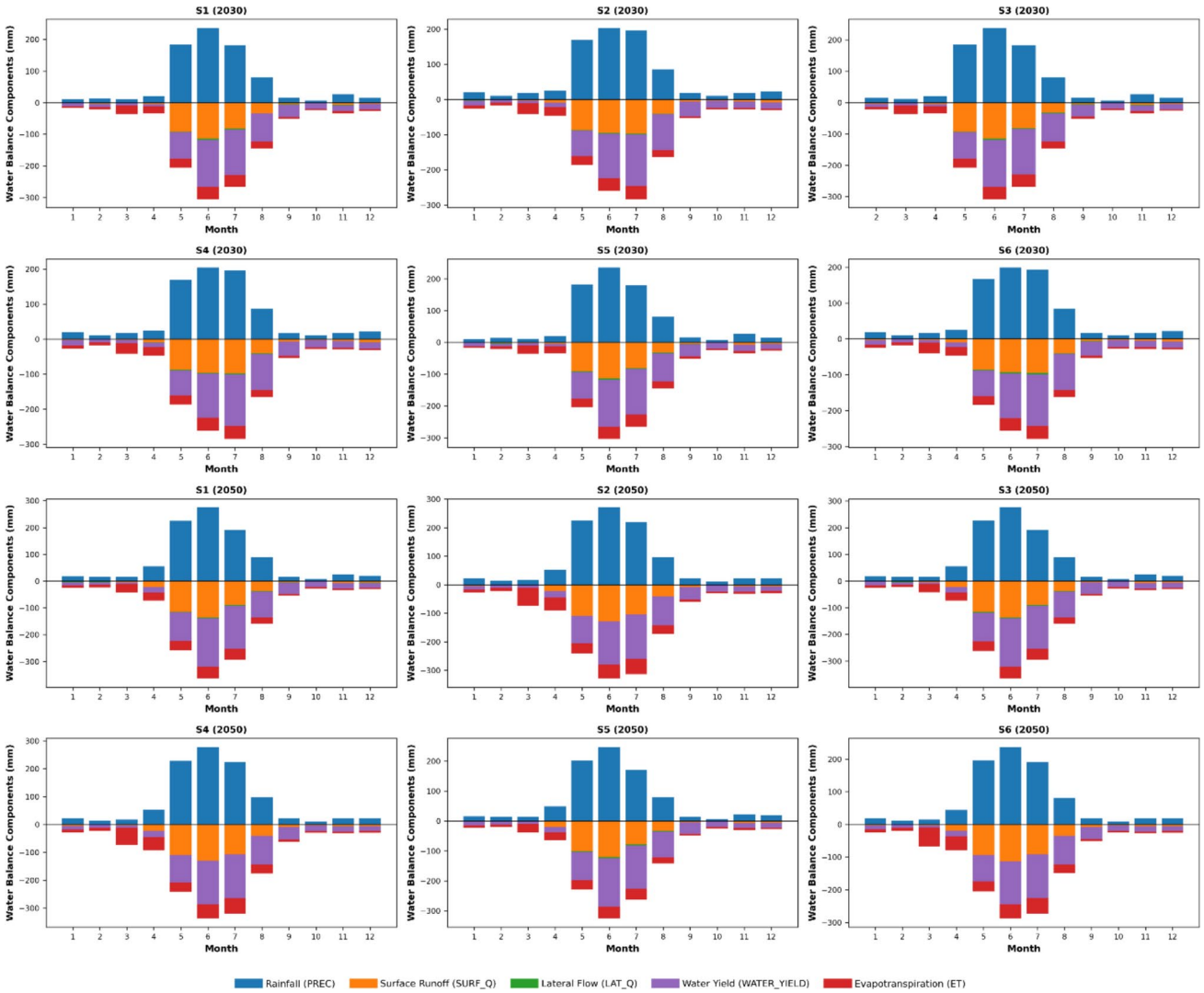

Fig. 7 Water balance components for the developed scenarios

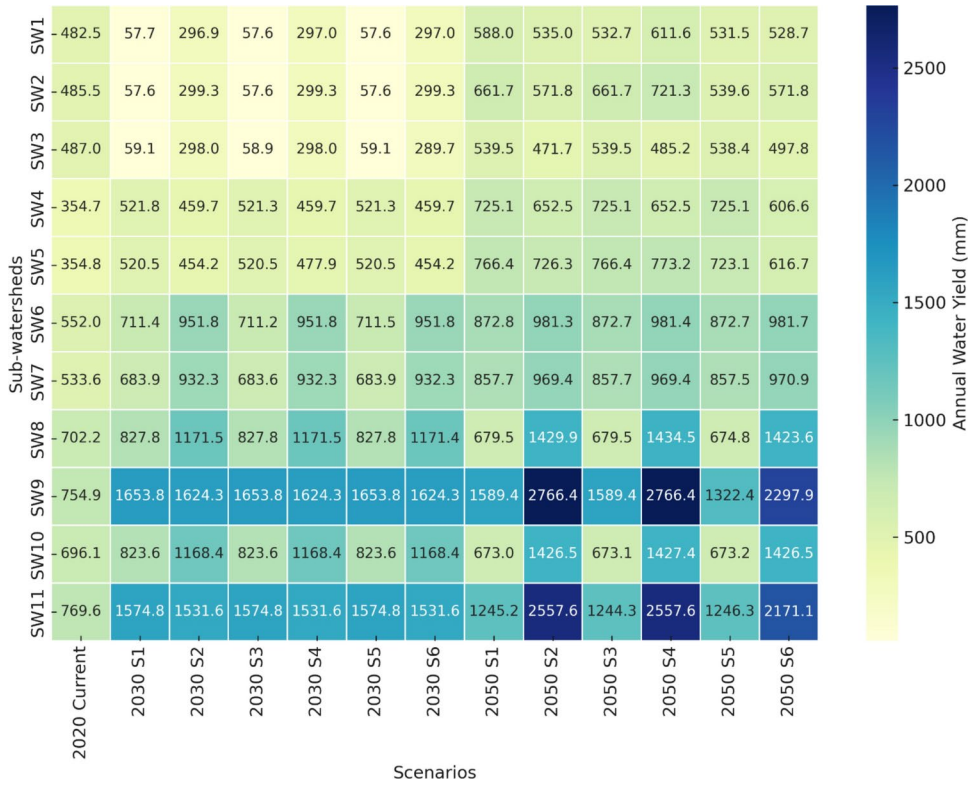

Fig. 8 Annual water yields from sub-watersheds under different scenarios

457.75 mm and 420.24 mm, respectively. The valuation mirrored this pattern, with Aligarh leading at 866.46 million USD (MUSD), followed by Mirzapur at 976.24 MUSD, Bulandshahr at 438.49 MUSD, and Meerut at 239.52 MUSD. In 2030, under scenario S_3, water yield and valuation decreased by a small amount when compared to S_1. In Aligarh, water yield decreased by a minuscule amount of 0.09% to 1024.49 mm, and so the valuation to 822.89 MUSD. For Mirzapur, nearly no difference in water yield (2007.92 mm) was observed leaving the valuation largely unchanged (1997.66 MUSD). For Meerut and Bulandshahr, water yield decreased by a minuscule amount of 0.05% and 0.23%, respectively which is also reflected in their respective valuation which are 28.62 and 60.20 MUSD. Similarly, in scenario S_5, the changes were also very small. In Aligarh water yield decreased slightly by 0.08% to 1024.66 mm, leading to a similar valuation decrement of 0.08% to 823.02 MUSD, while for Mirzapur no changes were observed in water yield, hence neither in the valuation. For Meerut and Bulandshahr, a curtailment in the water yield of 0.05% to 50.21 mm and 0.01% to 62.65 mm is perceived. When collating S_4 to S_2, for Aligarh and Meerut a slim increase in water yield of 0.64% and 0.01% is observed, while for Bulandshahr and Mirzapur no changes in the water yield were witnessed. On comparing S_6 to S_2, a decrement in water yield of 2.31% and 0.64% was observed for Bulandshahr and Aligarh, while for Meerut an increment of 0.01% was detected. For Mirzapur, water yield largely remains unaffected. In 2050, the trend of reductions continued under scenario S_3 when compared to S_1, where a reduction in water yield by 9.41%, 0.49%, and 0.08% was noted for Meerut, Bulandshahr, and Mirzapur. Aligarh with its water yield of 1828.27 mm didn't display any changes. On comparing S_5 to S_1, a decrement of 9.62%, 2.81%, and 0.76% was observed for Meerut, Bulandshahr, and Aligarh, respectively. Only for Mirzapur, a slight improvement of 0.09% which translates to 1589.02 mm of water yield was observed. On comparing S_4 to S_2, an improvement in water yield of 14.34%, 6.09%, and 1.56% was perceived for Meerut, Bulandshahr, and Aligarh, while for Mirzapur it remains essentially the same. On evaluating S_6 to S_2 a decrease in water yield of 1.17%, 5.03%, and 15.11% is noticed for Meerut, Aligarh, and Mirzapur, while for Bulandshahr an increment of 4.26% is detected. These alterations were primarily attributed to the spatial variation in precipitation of the climatic projections and dominant soil & land use type in the target districts along with the localized effects of OF and AgF over the hydrological response. Figure 9 depicts the surface plot of annual water yield along with its valuation for the target districts.

The study revealed modest changes in water yield under different land-use policy scenarios (BaU, Optimistic, and Pessimistic) across 2030 and 2050 projections. While previous studies have documented positive hydrological effects of OF and AgF, the findings of this study indicate localized rather than basin-wide impacts. This finds alignment with

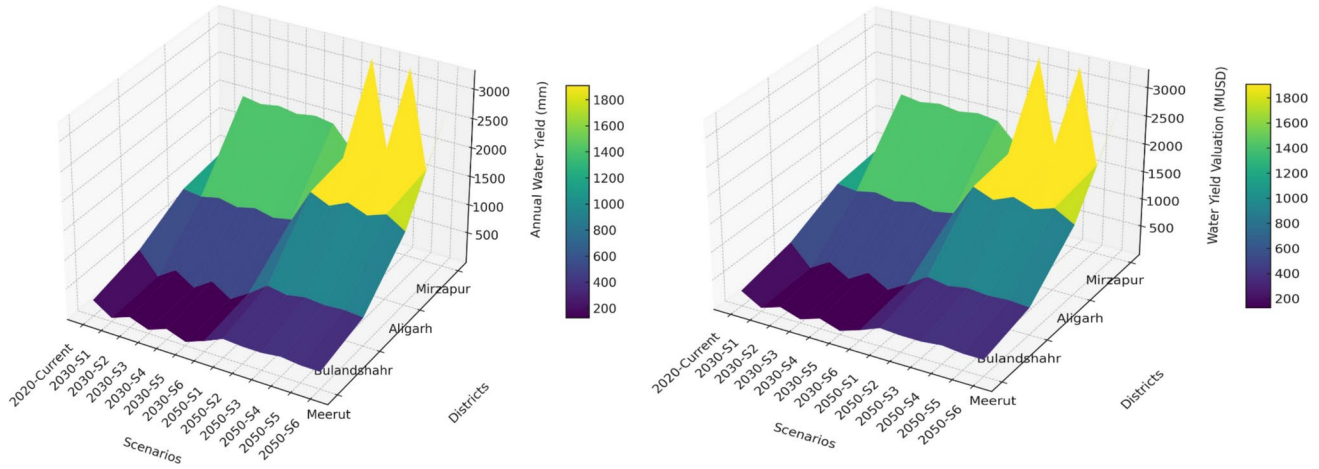

Fig. 9 Annual water yield and its valuation for the target districts

earlier studies that, suggested that land-use transitions influence water yield at the micro-watershed level, but the effects are often diluted and do not always translate into significant changes at basin-wide water balance scales (Kiersch 2000; Schilling & Libra 2003; Ghaffari et al. 2010; Winchell et al. 2013). This indicates that while OF and AgF can enhance soil moisture retention and infiltration at the field scale, their large-scale hydrological impacts remain context-dependent, emphasizing the need for spatially adaptive water management strategies. Moreover, the regional variability of precipitation, soil type, and vegetation cover plays a crucial role in determining the net impact of OF and AgF on hydrological processes. The study's insights also find application beyond the UGB to other monsoon-driven river basins, such as the Brahmaputra River in India, Indus in India & Pakistan (Laghari et al. 2012), and Murray-Darling in Australia (Grafton et al. 2014), where CC impacts are expected to alter water availability and seasonal flow patterns.

The study also underscores critical implications for hydrology, policy, and economic valuation suggesting that the climate-induced hydrological variability may overshadow land-use effects, making CC adaptation a priority. The results also highlight the importance of soil type in modulating hydrological response, as seen in the contrast between SW9 and SW11, where higher infiltration indices due to different soil types resulted in greater groundwater contribution. Additionally, it reinforces the need for watershed-scale conservation planning rather than localized land-use interventions to achieve significant hydrological improvements. The findings also support policy integration of climate-resilient agriculture, aligning with India's Jal Shakti Mission and Namami Gange initiative. The economic valuation underscores variability among districts, necessitating tailored interventions. For instance, districts with higher water yields might benefit from policies that enhance water conservation, while areas with lower yields could prioritize agroforestry for improved soil–water dynamics (Verma et al. 2017). Further, integrating adaptive land-use strategies with advanced climate projections is critical for future hydrological planning (Kundzewicz et al. 2007). To have a significant hydrological impact OF and AgF are needed to be scaled up substantially across larger regions. Also, expanding OF and AgF requires financial incentives, community engagement, and long-term policy frameworks, given that localized hydrological benefits alone may not be sufficient to drive widespread adoption. This ties into challenges related to policy incentives, land ownership patterns, and farmer buy-in (Loren and Lal 2016). Incentivizing OF and AgF adoption through government subsidies & community-driven programs and linking hydrological outcomes with socio-economic benefits to provide a more holistic view can support this endeavor. Finally, establishing datasets that evaluate the impacts of OF and AgF over larger timescales (say several decades) would benefit the cause (Rahman et al. 2023). Though the study is explicit in terms of quantifying the hydrologic response it has several limitations as well. These include (i) Short-term modeling horizon (2020–2050) for observing hydrological impacts of land-use transitions as they often require longer timescales to fully manifest, (ii) Simplified economic valuation of water yield assuming uniform pricing which may not account for region-specific socio-economic conditions, variations in water accessibility, and competing water demands, (iii) Exclusion of social and policy dimensions (not considering the socio-political barriers such as land ownership patterns, farmer incentives, and institutional support, to scaling up OF and AgF practices), and (iv) Reliance on a single GCM for RCP projections, which, while robust, does not account for inter-model variability and might introduce bias to the results of the hydrologic modeling. A longer projection period with multi-model ensembles to reduce bias could improve projection reliability and provide a more comprehensive assessment.

Further, future research could integrate spatially explicit hydro-economic models to refine water valuation estimates. Additionally, addressing socio-political barriers to OF and AgF expansion and integrating stakeholder-based scenario planning could enhance the policy relevance of hydrological modeling efforts. Addressing these limitations will further enhance the accuracy and applicability of hydrological predictions, making the findings more actionable for policymakers and water managers.

Conclusion and recommendations

This study has thoroughly evaluated the hydrological responses of the USGCM sub-basin in the UGB, considering both current and future land use and CC scenarios using the SWAT model integrated with GCMs. The study revealed that while OF and AgF practices are thought to have a positive influence over hydrological dynamics, their actual impact on water yield remains minimal, especially over shorter timescales. This limited impact is attributed to the small scale of land transitioning to OF and AgF, the spatial concentration of these practices, and the dominant influence of climate variables over land use changes. Further, the economic valuation of water yield across different districts underscores the importance of localized factors such as soil type, land use distribution, and specific precipitation patterns, which collectively govern the hydrological outcomes more significantly than broader land use policies alone. The findings highlight the complexity of predicting hydrological responses in the face of multiple interacting factors, suggesting that current land use changes may not be sufficient to drive significant alterations in hydrological patterns within the timeframe of the study. Given the findings, several recommendations emerge for future water resource management and policy development. These include (i) Scaling up sustainable practices to produce substantial hydrological impacts with policies aiming to expand these practices across larger areas, especially in critical zones identified as highly sensitive to variations in water yield, (ii) District-specific interventions as the heterogeneity in hydrological responses across different districts suggests that one-size-fits-all policies may be less effective suggesting for tailored interventions, (iii) Integration of advanced and localized climate projections for the development of future water resource management strategies, (iv) Continuous monitoring and adaptive management via establishing a long-term monitoring framework to assess the ongoing impacts of land use changes and climate variability on water resources, and (v) Integration with socio-economic models to provide a more holistic understanding of how human activities influence water resources and exploring the trade-offs between economic development and environmental sustainability. By addressing these areas, future research can contribute to more effective water resource management strategies that are resilient to the complex and evolving challenges posed by CC and land use dynamics.

Supplementary Information The online version contains supplementary material available at https://doi.org/10.1007/s40899-025-01228-1.

Acknowledgements The authors gratefully acknowledge TEEB-UNEP, Nairobi. Further, the authors also extend their acknowledgment to facilities and support received from the Director, ICAR-Indian Institute of Farming Systems Research, Modipuram, India.

Author contributions Meraj Alam Ansari: Conceptualization, investigation, monitoring, data curation, writing of original and final draft, review & editing, and project administration; Natesan Ravisankar: Conceptualization, investigation, visualization, review & editing, and project administration; Himanshu Joshi: Data curation, data analysis, modelling, writing of first and final draft, and review & editing; Meenu Rani: Data curation, data analysis, and review & editing; Mohammad Shamim: Conceptualization, Investigation, data analysis, and review & editing; Adlul Islam: Review and editing, visualization, and data analysis; Ashisa K. Prusty: Investigation, data curation, and review & editing; Raghavendra K.J.: Investigation and review & editing; Raghuveer Singh: Investigation and review & editing; Sunil Kumar: Conceptualization, review & editing, and project administration; Azad S. Panwar: Conceptualization, review & editing, and project administration.

Funding The authors are grateful to TEEB-UNEP, Nairobi for financial support for possible publication under the project 'TEEB Agri-Food Initiatives in Uttar Pradesh' (SSFA/2021/4738).

Data availability The data used in this study is publicly available from open sources. All datasets can be accessed through the respective platforms or repositories. Detailed information and links to the sources of data used in this analysis are provided in the methods section of the manuscript.

Declarations

Conflict of interest The authors declare that they have no conflict of interest.

Ethical approval The authors concede that to the best of their knowledge, the submitted manuscript has no conceivable ethical contentions. Further, no known personal relationship has appeared to influence the deliberated study under the contemplated manuscript.

References

Abbaspour KC, Rouholahnejad E, Vaghefi S, Srinivasan R, Yang H, Kløve B (2015) A continental-scale hydrology and water quality model for Europe: Calibration and uncertainty of a high-resolution large-scale SWAT model. J Hydrol 524:733–752. https://doi.org/10.1016/j.jhydrol.2015.03.027

Abbaspour KC, Vejdani M, Haghighat S (2007) SWAT-CUP calibration and uncertainty programs for SWAT. In: Modsim international congress on modelling and simulation. Modelling and

simulation society of Australia and New Zealand, pp: 1596–1602. https://doi.org/10.36334/modsim.2007.L12.abbaspour

Abbaspour KC (2015) SWAT-CUP: SWAT calibration and uncertainty program-A user manual. swiss federal institute of aquatic science and technology, Dübendorf, Switzerland, 100 p. swat.tamu.edu/media/114860/usermanual_swatcup.pdf

Allan JD (2004) Landscapes and riverscapes: the influence of land use on stream ecosystems. Ann Rev Ecol, Evol Syst 35:257–284. https://doi.org/10.1146/annurev.ecolsys.35.120202.110122

Altaf F, Meraj G, Romshoo SA (2013) Morphometric analysis to infer hydrological behavior of Lidder watershed, Western Himalaya, India. Geogr J Hindawi 2013:178021. https://doi.org/10.1155/2013/178021

Arnold CL, Gibbons CJ (1996) Impervious surface coverage: The emergence of a key environmental indicator. J Ameri Plann Assoc 62(2):243–258. https://doi.org/10.1080/01944369608975688

Arnold JG, Srinivasan R, Muttiah RS, Williams JR (1998) Large area hydrologic modeling and assessment part I: Model development. J Ameri Water Resour Asso 34(1):73–89. https://doi.org/10.1111/j.1752-1688.1998.tb05961.x

Arnold JG, Moriasi DN, Gassman PW, Abbaspour KC, White MJ, Srinivasan R et al (2012) SWAT: Model use, calibration, and validation. Trans ASABE 55(4):1491–1508. https://doi.org/10.13031/2013.42256

Arthington AH, Bunn SE, Poff NL, Naiman RJ (2006) The challenge of providing environmental flow rules to sustain river ecosystems. Ecol Appli 16(4):1311–1318. https://doi.org/10.1890/1051-0761(2006)016[1311:tcopef]2.0.co;2

Azarbad H (2022) Conventional vs. organic agriculture-which one promotes better yields and microbial resilience in rapidly changing climates? Front Microbio 13:903500. https://doi.org/10.3389/fmicb.2022.903500

Čerkasova N, White M, Arnold J, Bieger K, Allen P, Gao T et al (2023) Field scale SWAT+ modeling of corn and soybean yields for the contiguous United States: National Agroecosystem Model Development. Agricult Syst 210:103695. https://doi.org/10.1016/j.agsy.2023.103695

CGWB (2006) Watershed Atlas of India, Central Ground Water Board, Ministry of Water Resources, Govt. of India, New Delhi

Chang M (2013) Forest hydrology: an introduction to water and forests. CRC Press, Taylor & Francis Group, Boca Raton, Florida, USA

Chen J, Chang H (2020) Relative impacts of climate change and land cover change on streamflow using SWAT in the Clackamas River Watershed, USA. J Water Climate Change 12:1454–1470. https://doi.org/10.2166/wcc.2020.123

Chen G, Li X, Liu X (2020) Global land projection based on plant functional types with a 1-km resolution under socio-climatic scenarios. Scient Data 9:125. https://doi.org/10.1038/s41597-022-01208-6

Chow VT, Maidment DR, Mays LW (1988) Applied hydrology. McGraw-Hill Inc, New York

Cloke HL, Pappenberger F (2009) Ensemble flood forecasting: A review. J Hydrol 375(3–4):613–626. https://doi.org/10.1016/j.jhydrol.2009.06.005

Ficklin DL, Luo Y, Stewart IT, Maurer EP (2012) Development and application of a hydroclimatological stream temperature model within the Soil and Water Assessment Tool. Water Res Res 48:101515. https://doi.org/10.1029/2011WR011256

Foley JA, DeFries R, Asner GP, Barford C, Bonan G, Carpenter SR et al (2005) Global consequences of land use. Science 309(5734):570–574. https://doi.org/10.1126/science.1111772

Gassman PW, Reyes MR, Green CH, Arnold JG (2007) The soil and water assessment tool historical development, applications, and future research directions. Trans ASABE 50(4):1211–1250. https://doi.org/10.13031/2013.23637

Ghaffari G, Keesstra S, Ghodousi J, Ahmadi H (2010) SWAT-simulated hydrological impact of land-use change in the Zanjanrood basin. Northwest Iran Hydrolo Processes 24(7):892–903. https://doi.org/10.1002/hyp.7530

Grafton RQ, Pittock J, Williams J et al (2014) Water planning and hydro-climatic change in the Murray-Darling Basin, Australia. Ambio 43:1082–1092. https://doi.org/10.1007/s13280-014-0495-x

Gupta HV, Kling H, Yilmaz KK, Martinez GF (2009) Decomposition of the mean squared error and NSE performance criteria: implications for improving hydrological modelling. J Hydrol 377(1–2):80–91. https://doi.org/10.1016/j.jhydrol.2009.08.003

Haleem K, Khan AU, Ahmad S, Khan MZ, Khan FA, Khan WM et al (2022) Hydrological impacts of climate and land-use change on flow regime variations in upper Indus basin. J Water Climate Change 13:758–770. https://doi.org/10.2166/wcc.2021.238

Hirsch RM, Ryberg KR (2012) Has the magnitude of floods across the USA changed with global CO_2 levels? Hydrolo Sci J 57(1):1–9. https://doi.org/10.1080/02626667.2011.621895

Hyandye C, Worqul A, Martz LW, Muzuka ANN (2018) The impact of future climate and landuse/cover change on water resources in the Ndembera watershed and their mitigation and adaptation strategies. Environ Syst Res 7:7. https://doi.org/10.1186/s40068-018-0110-4

ICAR-CAFRI (2016) Annual report. ICAR-Central Agroforestry Research Institute Gwalior Road, Jhansi, India, 100 p

ICAR-IIFSR (2021) Annual report. ICAR-Indian Institute of Farming Systems Research, Modipuram, Meerut, India

Immerzeel WW, van Beek LPH, Bierkens MFP (2010) Climate change will affect the Asian water towers. Science 328(5984):1382–1385. https://doi.org/10.1126/science.1183188

Jain, SK, Jain SK, Jain N, Xu CY (2017) Hydrologic modeling of a Himalayan Mountain basin by using the SWAT model. Hydrol Earth Syst Sci Dis [preprint]. https://doi.org/10.5194/hess-2017-100

Jose S (2009) Agroforestry for ecosystem services and environmental benefits: an overview. Agrofor Syst 76(1):1–10. https://doi.org/10.1007/s10457-009-9229-7

Kiersch B (2000) Land use impacts on water resources: a literature review. Land and Water Development Division, FAO of UN, Rome, 12 p

Krysanova V, Arnold JG (2008) Advances in ecohydrological modelling with SWAT-a review. Hydrolo Sci J 53(5):939–947. https://doi.org/10.1623/hysj.53.5.939

Kumar S, Kushwaha SPS (2013) Modelling soil erosion risk based on RUSLE-3D using GIS in a Shivalik sub-watershed. J Earth Syst Sci 122:389–398. https://doi.org/10.1007/s12040-013-0276-0

Kumar M, Denis DM, Kundu A, Joshi N, Suryavanshi S (2022) Understanding land use/land cover and climate change impacts on hydrological components of Usri watershed India. App Water Sci. https://doi.org/10.1007/s13201-021-01547-6

Kundzewicz ZW, Mata LJ, Arnell NW, Döll P, Kabat P, et al. (2007) Freshwater resources and their management. Climate Change 2007: Impacts, adaptation and vulnerability. Contribution of Working Group II to the Fourth assessment report of the intergovernmental panel on climate change, pp: 173–210

Laghari AN, Vanham D, Rauch W (2012) The Indus Basin in the framework of current and future water resources management. Hydrol Earth Syst Sci 16(4):1063–1083. https://doi.org/10.5194/hess-16-1063-2012

Lai G, Luo J, Li Q, Qiu L, Pan R, Zeng X et al (2020) Modification and validation of the SWAT model based on multi-plant growth mode, a case study of the Meijiang River Basin. China J Hydrol 585:124778. https://doi.org/10.1016/j.jhydrol.2020.124778

Lorenz K, Lal R (2016) Environmental impact of organic agriculture. Advances Agron 139:99–152. https://doi.org/10.1016/bs.agron.2016.05.003

Loucks DP, Van Beek E (2005) Water resources systems planning and management: an introduction to methods, models, and applications. UNESCO Publishing

Lüke A, Hack J (2018) Comparing the applicability of commonly used hydrological ecosystem services models for integrated decision-support. Sustainability 10:346. https://doi.org/10.3390/su10020346

Mishra V, Kumar D, Ganguly AR, Sanjay J, Mujumdar M, Krishnan R et al (2014) Reliability of regional and global climate models to simulate precipitation extremes over India. J Geophy Res 119(15):9301–9323. https://doi.org/10.1002/2014JD021636

Montagnini F (2024) Introduction. Challenges and Achievements in Agroforestry in the New Millennium. In: Montagnini F (Eds.) Integrating landscapes: agroforestry for biodiversity conservation and food sovereignty. Advances in agroforestry. Springer, Cham. https://doi.org/10.1007/978-3-031-54270-1_1

Moriasi DN, Arnold JG, Van Liew MW, Bingner RL, Harmel RD, Veith TL (2007) Model evaluation guidelines for systematic quantification of accuracy in watershed simulations. Trans of the ASABE 50(3):885–900. https://swat.tamu.edu/media/90109/moriasimodeleval.pdf

Mosbahi M, Kassouk Z, Benabdallah S, Aouissi J, Arbi R, Mrad M et al (2023) Modeling hydrological responses to land use change in Sejnane Watershed northern Tunisia. Water 15:1737. https://doi.org/10.3390/w15091737

Neitsch SL, Arnold JG, Kiniry JR, Williams JR (2011) Soil and water assessment tool theoretical documentation version 2009. Grassland, soil and water research laboratory, Temple, Texas, USA

Niraula R, Meixner T, Norman LM (2015) Determining the importance of model calibration for forecasting absolute/relative changes in streamflow from LULC and climate changes. J Hydrol 522:439–451. https://doi.org/10.1016/j.jhydrol.2015.01.007

Parajuli PB, Ouyang Y (2013) Watershed-scale hydrological modeling methods and applications. In: Paul Bradley (Ed.) Current Perspective in Contaminant Hydrology and Water Resource Sustainability. IntechOpen, London

Pickett ST, Cadenasso ML, Grove JM (2004) Resilient cities: meaning, models, and metaphor for integrating the ecological, socio-economic, and planning realms. Landsc Urban Plann 69(4):369–384. https://doi.org/10.1016/j.landurbplan.2003.10.035

Rahman MH, Ahrends HE, Raza A, Gaiser T (2023) Current approaches for modeling ecosystem services and biodiversity in agroforestry systems: challenges and ways forward. Front Forest Global Change 5:1032442. https://doi.org/10.3389/ffgc.2022.1032442

Rostamian R, Jaleh A, Afyuni M, Mousavi SF, Heidarpour M, Jalalian A, Abbaspour KC (2008) Application of a SWAT model for estimating runoff and sediment in two mountainous basins in central Iran. Hydrol Sci J 53(5):977–988. https://doi.org/10.1623/hysj.53.5.977

Santosha YT, Kurniasih B, Alam T, Handayani S, Supriyanta AA et al (2024) Investigating the dynamics of upland rice (*Oryzasativa* L.) in rainfed agroecosystems: an in-depth analysis of yield gap and strategic exploration for enhanced production. Front Sustain Food Syst 8:1384530. https://doi.org/10.3389/fsufs.2024.1384530

Schilling KE, Libra RD (2003) Increased baseflow in Iowa over the second half of the 20th century. J Ameri Water Res Associ 39(4):851–860. https://doi.org/10.1111/j.1752-1688.2003.tb04410.x

Schuol J, Abbaspour KC, Yang H et al (2008) Modeling blue and green water availability in Africa. Water Resour Res 44(7):W07406. https://doi.org/10.1029/2007WR006609

Sharmila S, Susmitha J, Sahai AK, Abhilash S, Chattopadhyay R (2015) Future projection of Indian summer monsoon variability under climate change scenario: an assessment from CMIP5 climate models. Global Planeta Change 124:62–78. https://doi.org/10.1016/j.gloplacha.2014.11.004

Sheffield J, Wood EF, Roderick ML (2012) Little change in global drought over the past 60 years. Nature 491(7424):435–438. https://doi.org/10.1038/nature11575

Singh L, Saravanan S (2020) Simulation of monthly streamflow using the SWAT model of the Ib River watershed, India. Hydro Res 3:95–105. https://doi.org/10.1016/j.hydres.2020.09.001

Smith M, Burgess SSO, Suprayogo D, Lusiana B, Widianto W (2004) Uptake, partitioning and redistribution of water by roots in mixed-species agroecosystems. In: Van Noordwijk M, Cadisch G, Ong, CK (Eds.) Below-ground Interactions in Tropical Agroecosystems: Concepts and Models with Multiple Plant Components, CABI, pp: 157–170. https://doi.org/10.1079/9780851996738.0157

Soman A, Chithra NR (2019) Impacts of climate change on irrigated agriculture in the chaliyar river basin in Kerala, India. Int J Big Data Mining Global Warm 01:1950001. https://doi.org/10.1142/S2630534819500013

Tadesse AA, Arnold J, Jeong J, Jones A, Srinivasan R (2023) Innovative approach to prognostic plant growth modeling in SWAT+ for forest and perennial vegetation in tropical and Sub-Tropical climates. J Hydrol X 20(1):100156. https://doi.org/10.1016/j.hydroa.2023.100156

Trenberth KE, Dai A, Rasmussen RM, Parsons DB (2003) The changing character of precipitation. Bull Ameri Meteorol Soc 84(9):1205–1217. https://doi.org/10.1175/BAMS-84-9-1205

Tuppad P, Douglas-Mankin KR, Lee T, Srinivasan R, Arnold JG (2011) Soil and water assessment tool (SWAT) hydrologic/water quality model: extended capability and wider adoption. Trans ASABE 54(5):1677–1684. https://doi.org/10.13031/2013.39856

Verma M, Negandhi D, Khanna C, Edgaonkar A, David A, Kadkodi G et al (2017) Making the hidden visible: economic valuation of tiger reserves in India. Ecosystem Ser 26(A):235–244. https://doi.org/10.1016/j.ecoser.2017.05.006

Wagner PD, Kumar S, Fiener P, Schneider K (2011) Hydrological modeling with SWAT in a monsoon-driven environment: experience from the Western Ghats, India. Trans ASABE 54(5):1783–1790. https://doi.org/10.13031/2013.39846

Wilhite DA (2000) Drought as a natural hazard: concepts and definitions. In Drought: a global assessment. Routledge

Winchell M, Srinivasan R, Di Luzio M, Arnold JG (2013) Arcswat Interface for SWAT2012: User's Guide. Blackland Research Center, Texas AgriLife Research, College Station, pp. 1–464

Wu Q, Xiong K, Li R, Xiao J (2023) Farmland hydrology cycle and agronomic measures in agroforestry for the efficient utilization of water resources under karst desertification environments. Forests 14(3):453. https://doi.org/10.3390/f14030453

Yuan Y, Nie W, Sanders E (2015) Problems and prospects of SWAT model application on an arid/semi-arid watershed in Arizona. In: Proceedings of the 2015 SEDHYD conference, Reno, NV, USA, pp. 19–23.

Zhang L, Zhang N, Yu W, Ge Y (2015) Hydrological responses to land-use change scenarios under constant and changed climatic conditions. Environ Manage 57:412–431. https://doi.org/10.1007/s00267-015-0620-z

Zhang H, Wang B, Li Liu D, Zhang M, Leslie LM, Yu Q (2020) Using an improved SWAT model to simulate hydrological responses to land use change: a case study of a catchment in tropical Australia. J Hydrol 585:124822. https://doi.org/10.1016/j.jhydrol.2020.124822